

$\mu$ -ARPES study of the kagome superconductor CsV<sub>3</sub>Sb<sub>5</sub>Kosuke NAKAYAMA<sup>1,2,\*</sup>, Yongkai LI<sup>3,4</sup>, Takemi KATO<sup>1</sup>, Min LIU<sup>3,4</sup>, Zhiwei WANG<sup>3,4</sup>,  
Takashi TAKAHASHI<sup>1,5,6</sup>, Yugui YAO<sup>3,4</sup>, and Takafumi SATO<sup>1,5,6,7,\*\*</sup><sup>1</sup>Department of Physics, Graduate School of Science, Tohoku University, Sendai 980-8578, Japan<sup>2</sup>Precursory Research for Embryonic Science and Technology (PRESTO),  
Japan Science and Technology Agency (JST), Tokyo 102-0076, Japan<sup>3</sup>Centre for Quantum Physics, Key Laboratory of Advanced Optoelectronic Quantum Architecture  
and Measurement (MOE), School of Physics, Beijing Institute of Technology, Beijing 100081, China<sup>4</sup>Beijing Key Lab of Nanophotonics and Ultrafine Optoelectronic Systems, Beijing Institute of  
Technology, Beijing 100081, China<sup>5</sup>Center for Spintronics Research Network, Tohoku University, Sendai 980-8577, Japan<sup>6</sup>Advanced Institute for Materials Research (WPI-AIMR), Tohoku University, Sendai 980-8577, Japan<sup>7</sup>International Center for Synchrotron Radiation Innovation Smart, Tohoku University, Sendai 980-8577, Japan

## 1 Introduction

Recently, a family of AV<sub>3</sub>Sb<sub>5</sub> (A = K, Rb, and Cs) was discovered to be a kagome superconductor with superconducting transition temperature  $T_c$  of 0.93–2.5 K, despite the fact that kagome metals rarely become a superconductor. Besides superconductivity, AV<sub>3</sub>Sb<sub>5</sub> commonly undergoes a charge-density wave (CDW) transition at  $T_{CDW} = 78$ –103 K accompanied with three-dimensional (3D)  $2 \times 2 \times 2$  charge order. While overall electronic structure of AV<sub>3</sub>Sb<sub>5</sub> has been almost established, the mechanism of superconductivity and CDW is highly controversial. While the several different unconventional superconductivity are proposed by theory, the conventional vs unconventional nature of superconductivity is far from reaching a consensus in the experiment, as represented by contradictory reports on the presence/absence of gap nodes. The electronic states relevant to the CDW formation are also under intensive debate. An apparent CDW-gap opening was not observed in previous ARPES studies, whereas scanning tunneling microscopy/spectroscopy (STM/STS) reported a gap opening. While the Peierls instability due to the Fermi surface (FS) nesting is suggested by theory and optical spectroscopy, x-ray scattering reports the absence of expected phonon anomaly. To clarify the low-energy electron excitation relevant to the superconductivity and CDW, we have performed  $\mu$ -ARPES experiment on CsV<sub>3</sub>Sb<sub>5</sub> single crystals [1].

## 2 Experiment

High-quality single crystals of CsV<sub>3</sub>Sb<sub>5</sub> were synthesized with the self-flux method. VUV-ARPES measurements with micro-focused synchrotron light were performed with a DA30 electron analyzer at BL28A [2], as well as SES2002 spectrometers at Tohoku University. SX-ARPES measurements were performed with a SES2002 analyzer at BL2. We used energy tunable photons of the VUV region ( $h\nu = 85$ –125 eV) at BL-28A and the SX region ( $h\nu = 230$ –350 eV) at BL-2A. The energy resolution was set to be at 35–100 meV. The angular resolution was

set to be 0.2–0.3°. Crystals were cleaved *in-situ* in an ultrahigh vacuum of  $\sim 1 \times 10^{-10}$  Torr.

## 3 Results and Discussion

Figure 1(a) shows energy distribution curves (EDCs) measured with synchrotron radiation in the VUV region at the normal-emission set up. One can recognize that the energy location of the band shows a systematic variation as a function of  $h\nu$  and such variation is also visualized in the second-derivative intensity plot in Fig. 1(b). From the periodicity of band dispersion together with the normal-emission ARPES data obtained with SX photons [Fig. 1(c)], we have estimated the inner-potential value to be  $V_0 = 10.0$  eV.

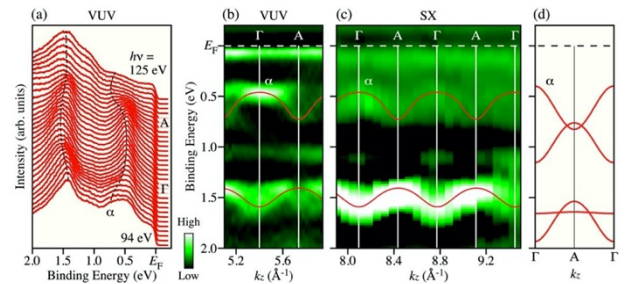


Fig. 1 (a)  $h\nu$  dependence of EDCs for CsV<sub>3</sub>Sb<sub>5</sub> measured in the normal-emission set up at  $T = 20$  K. (b) Second-derivative intensity of EDCs plotted as a function of  $k_z$  and binding energy ( $E_B$ ) obtained with VUV photons ( $h\nu = 94$ –125 eV). (c) Same as (b) but obtained with the SX photons ( $h\nu = 230$ –350 eV). (d) The calculated band structure along the  $k_z$  cut obtained with the first-principles band-structure calculations [1].

Figure 2(a) shows the ARPES-intensity map at representative binding energy ( $E_B$ ) slices as a function of  $k_x$  and  $k_y$ , obtained with 106-eV photons which probe the  $k_z \sim 0$  plane of the bulk BZ. One can identify a circular pocket

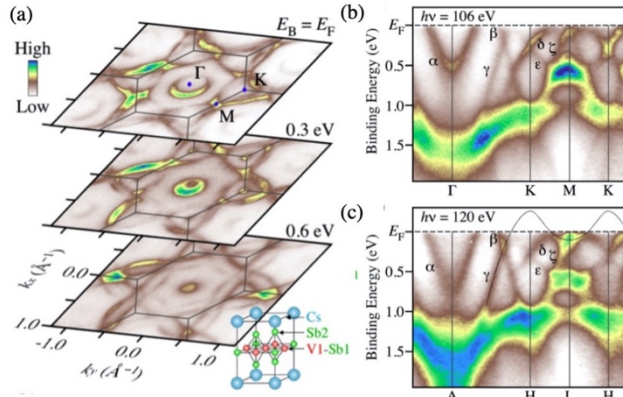


Fig. 2 (a) ARPES-intensity maps at binding energies ( $E_B$ 's) of  $E_F$ , 0.3 eV, and 0.6 eV plotted as a function of  $k_x$  and  $k_y$ , for  $\text{CsV}_3\text{Sb}_5$  measured at  $T = 20$  K with 106-eV photons. (b), (c) ARPES intensity as a function of wave vector and EB measured along the  $\Gamma\text{KM}$  ( $k_z = 0$ ) and  $\text{AHL}$  ( $k_z = \pi$ ) cuts, respectively [1].

centered at the  $\Gamma$  point. This pocket originates from an Sb-derived electron band (the  $\alpha$  band) as visible from the ARPES-intensity plot along the  $\Gamma\text{KM}$  cut in Fig. 2(b). According to the DFT calculations, this band is attributed to the  $5p_z$  band of Sb1 atoms embedded in the kagome-lattice plane [see inset to Fig. 2(a)]. One can recognize in Fig. 2(a) triangular shaped intensity pattern centered at each K point which connects to each other around the M point and forms a large hexagonal FS centered at the  $\Gamma$  point. As shown in Fig. 2(b), this pocket originates from a band located at 1 eV at the K point (the  $\beta$  band) that displays an overall linear dispersion toward  $E_F$  on approaching the  $\Gamma$  point and crosses  $E_F$  at  $k \sim 2/3$  of the  $\Gamma\text{K}$  interval. This band is attributed to the kagome-lattice band with mainly  $V-3d_{xy}$  character. This band intersects other two linearly dispersive bands ( $\gamma$  and  $\delta$  bands) at  $\sim 0.1$  eV and  $\sim 0.5$  eV, and the  $\delta$  band also intersects the linearly dispersive  $\epsilon$  band at the K point, forming multiple Dirac points. The  $\delta$  band rapidly disperses toward  $E_F$  on approaching the M point and participates in forming the saddle point. At the M point, there is another holelike band ( $\zeta$  band) with the top of the dispersion below  $E_F$ .

At  $h\nu = 120$  eV that corresponds to the  $k_z = \pi$  plane, there are several similarities in the band dispersions with those at the  $k_z = 0$  plane, e.g. linear dispersions of the  $\beta$ ,  $\gamma$ ,  $\delta$ , and  $\epsilon$  bands and their Dirac-cone formation [compare Figs. 2(b) and 2(c)]. Besides such similarities, one can recognize a clear difference in the energy position of the  $\alpha$ -band bottom, i.e., it is located at  $E_B \sim 0.5$  and 0.75 eV at  $k_z = 0$  and  $\pi$ , respectively. One can also find that a shallow electron pocket centered at the L point appears only at the  $k_z = \pi$  plane. According to the calculation, this band is connected to the  $\gamma$  band. The observed band structures including finite  $k$  dispersions reasonably agree with the bulk band calculation, supporting their bulk nature.

Based on the overall three-dimensional band structure, we have studied the fine electronic structure in the vicinity

of  $E_F$  with high-resolution ARPES [1]. We found an energy gap of 50–70 meV at the Dirac-crossing points of linearly dispersive bands, pointing to an importance of spin-orbit coupling. We also found a signature of strongly FS- and momentum-dependent CDW gap characterized by the larger energy gap of maximally 70 meV for a band forming a saddle point around the M point, the smaller (0–18 meV) gap for a band forming massive Dirac cones and a zero gap at the  $\Gamma/\text{A}$ -centered electron pocket. The observed highly anisotropic CDW gap which is enhanced around the M point signifies an importance of scattering channel connecting the saddle points, laying foundation for understanding the nature of CDW and superconductivity in  $\text{AV}_3\text{Sb}_5$ .

#### Acknowledgements

We thank S. Souma, M. Kitamura, K. Horiba and H. Kumigashira for their assistance in the ARPES experiments. This work was supported by JST-CREST (No. JPMJCR18T1), JST-PREST (No. JPMJPR18L7), JSPS KAKENHI Grants (No. No. JP17H01139 and No. JP18H01160). T. K. acknowledges support from GP-Spin at Tohoku University.

#### References

- [1] K. Nakayama, Y. Li, T. Kato, M. Liu, Z. Wang, T. Takahashi, Y. Yao, and T. Sato, *Phys. Rev. B* **104**, L161112 (2021).
- [2] M. Kitamura, S. Souma, A. Honma, D. Wakabayashi, H. Tanaka, A. Toyoshima, K. Amemiya, T. Kawakami, K. Sugawara, K. Nakayama, K. Yoshimatsu, H. Kumigashira, T. Sato, and K. Horiba, *Rev. Sci. Instrum.* **93**, 033906 (2022).

\* k.nakayama@arpes.phys.tohoku.ac.jp

\*\* t-sato@arpes.phys.tohoku.ac.jp